PLOS ONE

RESEARCH ARTICLE

Borrelia burgdorferi, the Lyme disease spirochete, possesses genetically-encoded responses to doxycycline, but not to amoxicillin

Timothy C. Saylor[1‡], Timothy Casselli[2‡], Kathryn G. Lethbridge[1¤], Jessamyn P. Moore[1], Katie M. Owens[1], Catherine A. Brissette[2], Wolfram R. Zückert[3], Brian Stevenson[1,4]*

1 Department of Microbiology, Immunology and Molecular Genetics, University of Kentucky, School of Medicine, Lexington, Kentucky, United States of America, **2** Department of Biomedical Sciences, School of Medicine and Health Sciences, University of North Dakota, Grand Forks, North Dakota, United States of America, **3** Department of Microbiology, Molecular Genetics and Immunology, University of Kansas Medical Center, Kansas City, Kentucky, United States of America, **4** Department of Entomology, University of Kentucky, Lexington, Kentucky, United States of America

¤ Current address: Thermo Fisher, Grand Island, New York, United States of America
‡ TCS and TC contributed equally to this work and are to be considered co-equal first authors.
* brian.stevenson@uky.edu

Citation: Saylor TC, Casselli T, Lethbridge KG, Moore JP, Owens KM, Brissette CA, et al. (2022) *Borrelia burgdorferi*, the Lyme disease spirochete, possesses genetically-encoded responses to doxycycline, but not to amoxicillin. PLoS ONE 17(9): e0274125. https://doi.org/10.1371/journal.pone.0274125

Editor: Nikhat Parveen, Rutgers New Jersey Medical School, UNITED STATES

Received: April 5, 2022

Accepted: August 22, 2022

Published: September 30, 2022

Peer Review History: PLOS recognizes the benefits of transparency in the peer review process; therefore, we enable the publication of all of the content of peer review and author responses alongside final, published articles. The editorial history of this article is available here: https://doi.org/10.1371/journal.pone.0274125

Data Availability Statement: Raw RNA-Seq data have been deposited in the NCBI GEO sequence

Abstract

Some species of bacteria respond to antibiotic stresses by altering their transcription profiles, in order to produce proteins that provide protection against the antibiotic. Understanding these compensatory mechanisms allows for informed treatment strategies, and could lead to the development of improved therapeutics. To this end, studies were performed to determine whether *Borrelia burgdorferi*, the spirochetal agent of Lyme disease, also exhibits genetically-encoded responses to the commonly prescribed antibiotics doxycycline and amoxicillin. After culturing for 24 h in a sublethal concentration of doxycycline, there were significant increases in a substantial number of transcripts for proteins that are involved with translation. In contrast, incubation with a sublethal concentration of amoxicillin did not lead to significant changes in levels of any bacterial transcript. We conclude that *B. burgdorferi* has a mechanism(s) that detects translational inhibition by doxycycline, and increases production of mRNAs for proteins involved with translation machinery in an attempt to compensate for that stress.

Introduction

Lyme disease (Lyme borreliosis) is caused by infection by the spirochete *Borrelia burgdorferi* sensu lato (hereafter referred to as *B. burgdorferi*, for simplicity). Early manifestations include an expanding annular rash (erythema migrans) along with fever, body aches, and other "flu-like" symptoms. If untreated, more significant symptoms may be seen, including arthritis, meningitis, atrioventricular nodal block, or cardiac arrest [1–3]. This spirochete is sensitive to many types of antibiotics, and human Lyme disease is frequently treated with either

read archive database, and given accession number GSE197338.

Funding: BS, WRZ: R03 AI133056, National Institutes of Health. The funders had no role in study design, data collection and analysis, decision to publish, or preparation of the manuscript. CAB: U54GM128729 and 2P20GM104360-06A1, National Institutes of Health. The funders had no role in study design, data collection and analysis, decision to publish, or preparation of the manuscript.

Competing interests: The authors have declared that no competing interests exist.

doxycycline or amoxicillin [1, 2, 4–6]. Doxycycline inhibits bacterial translation, and amoxicillin inhibits assembly of cell wall peptidoglycan.

Some species of bacteria respond to the presence of antibiotics by modulating their gene and protein expression levels in efforts to overcome those stresses [7–12]. For examples, increasing production of efflux pumps or altering the relative expression levels of proteins involved with cell wall synthesis. Those observations raise the possibility that the Lyme disease spirochete may possess mechanisms that modify bacterial physiology in response to antibiotic therapies. Assessment of that possibility could inform prescribed antibiotics and dosages. Understanding these compensatory mechanisms allows for informed treatment strategies, and could lead to the development of new and/or improved therapeutics.

Exposing *B. burgdorferi* to sub-lethal levels of β-lactams may result in the spirochetes producing membrane protrusions or acquiring a spherical shape [13–18]. In other bacterial species, treatment with low levels of β-lactam antibiotics leads to weakening of the cell wall and cytoplasmic distortion due to osmotic influx of water [19–22]. However, there is a pervading hypothesis in the literature and among some physicians that β-lactam-induced "round bodies" are a genetically-encoded response by *B. burgdorferi* to avoid antibiotic killing [16–18, 23–34].

To address these points, we cultured *B. burgdorferi* in concentrations of doxycycline or amoxicillin that impaired, but did not completely prevent, bacterial replication. Bacteria were thus metabolically active, so changes could be interpreted as indicative of ongoing responses. To assess whether any physiological changes were due to genetically encoded processes, relative levels of mRNAs were compared for each condition.

Material and methods

Effects of antibiotic concentrations on replication of cultured *B. burgdorferi*

Strain B31-MI16, an infectious clone of *B. burgdorferi* type strain B31, was grown at 35˚C to mid-exponential phase (3 x 10^7 bacteria/ml) in liquid BSK-II medium [35, 36]. Triplicate aliquots of the culture were diluted 1:100 into fresh BSK-II that contained either no antibiotic, or 0.1, 0.2, or 0.4 μg/ml doxycycline or amoxicillin (Sigma). Bacterial numbers in each culture were then counted using a Petroff-Hauser counting chamber and dark field microscopy, marking time point 0. All cultures were counted every 24 hours for the first four days and on the seventh day. Antibiotic susceptibility assays were performed twice.

Photomicrography

Aliquots of bacterial cultures were spread on glass slides, covered with coverslips, then visualized using dark field microscopy with a 40x objective lens. Images were recorded with a C-mounted Accu-scope Excelis HD camera using Captavision+ software. Bacterial lengths were determined by comparing their sizes against a reference stage micrometer, using Captavision + software. To quantify *B. burgdorferi* with membrane distortions after incubation for 24 h in 0.2 μg/ml of amoxicillin, bacteria in randomly selected fields were photographed, then assessed manually for presence of membrane perturbations. Due to variations in numbers of bacteria per field, 109 control bacteria and 110 amoxicillin-treated bacteria were assessed.

Preparation of cultures for RNA sequencing

A mid-exponential phase (3 x 10^7 bacteria/ml) 35˚C culture of *B. burgdorferi* clone B31-MI16 was used as 1:100 inoculum into 18 separate tubes of 20ml BSK-II broth. Six cultures were not given any antibiotic, 6 received doxycycline to a final concentration of 0.2 μg/ml, and 6

cultures received amoxicillin to a final concentration of 0.2 μg/ml. After 3 hours incubation at 35˚C, 3 cultures of each condition were harvested by centrifugation for 15 min at 8200xG at 4˚C, then frozen at -80˚C. The remaining cultures were similarly harvested and frozen after 24 hours incubation at 35˚C. Frozen *B. burgdorferi* were shipped on dry ice to ACGT Inc. (https://www.acgtinc.com) for RNA processing and sequencing.

RNA extraction and RNA sequencing (RNA-Seq)

Purification of RNA, preparation of libraries, and sequencing were performed by ACGT Inc. according to their standard protocols (https://www.acgtinc.com). Briefly, RNA was extracted from the bacterial pellets by using the Quick RNA-Microprep Kit (Zymo Research). RNA was evaluated with DeNovix and Nanodrop. An individual library was produced for each culture, using Zymo-Seq Ribofree Total RNA Library Kits (Zymo Research). Libraries were evaluated by Qubit and 2100 bioanalyzer to assess quality and quantity before sequencing. Sequencing was performed on Illumina NextSeq500 PE150. Runs were demultiplexed using bcl2fastq to obtain raw fastq files. Experimentally triplicated RNA-Seq produces robust data that do not require accompanying quantitative-reverse transcription PCR analyses [37].

Bioinformatics

Analysis of transcriptome sequencing (RNA-Seq) data were performed in house, essentially described previously [38–40]. Briefly, adapters were removed from the sequencing reads by Trimmomatic [41]. The reads were aligned and counted with a transcriptome reference compiled from the *B. burgdorferi* strain B31-MI genome (RefSeq numbers AE000783 to AE000794 and AE001575 to AE001584) by using Salmon v1.5.2 [42]. Reads were normalized and differential expression analysis was conducted using DEseq2 [43]. Genes were considered to have significantly different expression at Fold-Change ≥ 2, padj ≤ 0.05, basemean > 20.

Data generated from RNA sequencing analyses were visualized with R v.4.0.1 (https://www.R-project.org/) using ggplot2 (https://doi.org/10.1007/978-3-319-24277-4) for MA plots, pie charts, and bar graphs.

Raw RNA-Seq data have been deposited in the NCBI GEO sequence read archive database, and given accession number GSE197338.

Results and discussion

Study design overview

To determine appropriate sublethal concentrations of antibiotics, an infectious clone of *B. burgdorferi* type strain B31 was cultured in liquid BSK-II medium that included various concentrations of either doxycycline or amoxicillin. Numbers of bacteria were counted daily over a course of 7 days, with inclusion of all motile and immobile spirochetes. Counting the number of organisms enabled determination of the effects of antibiotic treatment on completion of cell division. Under these culture conditions, this strain was completely inhibited from replicating by 0.4 μg/ml amoxicillin, while the minimum inhibitory concentration of doxycycline was greater than 0.4 μg/ml (Fig 1). Consistent with our findings, prior studies determined that minimum inhibitory and minimum bactericidal concentrations of doxycycline were 0.25–4 and 4–16 μg/ml, respectively, for Lyme disease borreliae [44]. Reported minimum inhibitory and minimum bactericidal concentrations of amoxicillin were 0.015–0.25 and 0.25–0.5 μg/ml, respectively [44]. In our investigations, concentrations of 0.2 μg/ml doxycycline and amoxicillin were found to substantially inhibit, but not eliminate, *B. burgdorferi* duplication (Fig 1).

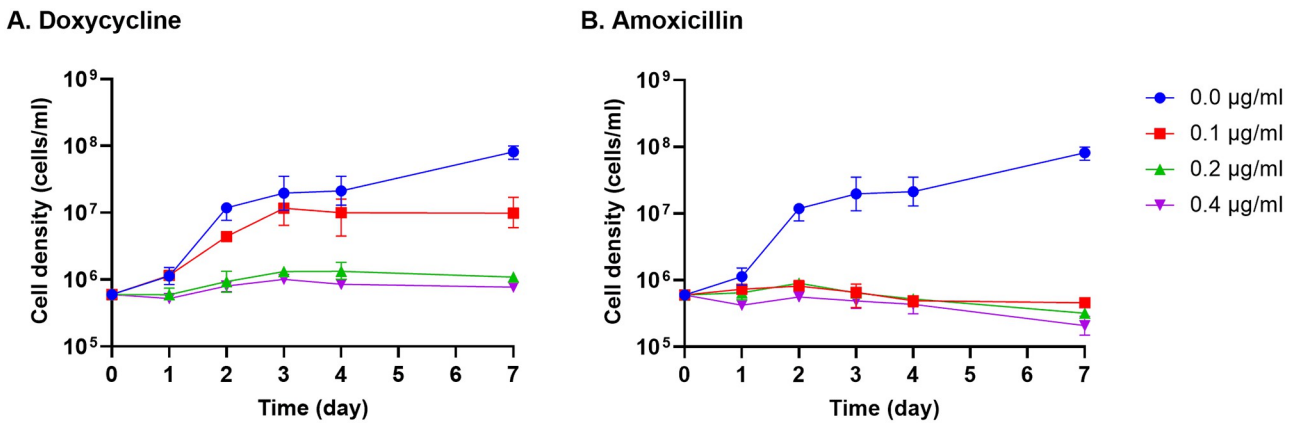

Fig 1. Effects of antibiotics on *B. burgdorferi* replication rates. (A) Doxycycline was added to freshly inoculated cultures at concentrations of 0.1 µg/mL, 0.2 µg/mL, and 0.4 µg/ml. (B) Amoxicillin was added to freshly inoculated cultures at concentrations 0.1 µg/mL, 0.2 µg/mL, and 0.4 µg/ml. Bacterial numbers were determined by microscopical examination with a Petroff-Hauser counting chamber after 1, 2, 3, 4 and 7 days of culture.

https://doi.org/10.1371/journal.pone.0274125.g001

Those concentrations were designated "sublethal", and were subsequently tested for their effects on cell morphology and gene expression in *B. burgdorferi*.

Cultures were then grown to mid-exponential phase (approximately 3 x 10^7 bacteria / ml), diluted 1:100 into aliquots of fresh media, then either no antibiotic, or 0.2 µg/ml of either doxycycline or amoxicillin were added. Cultures were incubated at 35˚C for either 3 or 24 hours prior to phenotype analysis. Longer time points were not examined, due to the increased possibility that substantial numbers of bacteria would die and their decaying RNA obscure results. To assess the effects of antibiotics on total gene expression, we took an unbiased approach using RNA sequencing (RNA-Seq). Effects of the antibiotics on bacterial morphologies were assessed by darkfield microscopy.

Under the sublethal concentrations of antibiotics used in our studies, bacteria continued to move, elongate, and divide, indicating that the spirochetes were metabolically active (Fig 1 and discussion below). These conditions allowed us to differentiate biological responses to antibiotics from experimental artefacts from dead and/or dying bacteria. On the other hand, two previous transcriptomic analyses of *B. burgdorferi* cultivated in antibiotics used concentrations of 50 µg/ml doxycycline [45, 46] or 50 µg/ml amoxicillin [45] for 5 days before RNA analyses. Those levels are 12 to 100-times greater than the minimum bactericidal concentrations [44]. Neither of those studies examined the physiology of *B. burgdorferi* during incubation under those conditions [45, 46].

Doxycycline induced gene expression changes associated with protein translation

Exposure of *B. burgdorferi* to 0.2 µg/ml doxycycline led to an initial significant decrease in expression of 36 genes after three hours compared to control cells without antibiotics (FoldChange ≥ 2, padj ≤ 0.05, basemean > 20), while no genes were significantly increased at this timepoint (Fig 2A; Table 1; S1 Table). Differentially expressed genes (DEGs) included those involved in protein translation, DNA replication/repair, cell motility, and carbohydrate metabolism, however only a small number of genes (≤ 7) from each pathway were affected (Fig 2B and 2C). Due to the low number of differentially expressed genes and the diversity of predicted functions, it is possible that these differences reflect nonspecific mRNA turnover differences in the presence of doxycycline. There are no obvious benefits to reducing levels of those transcripts.

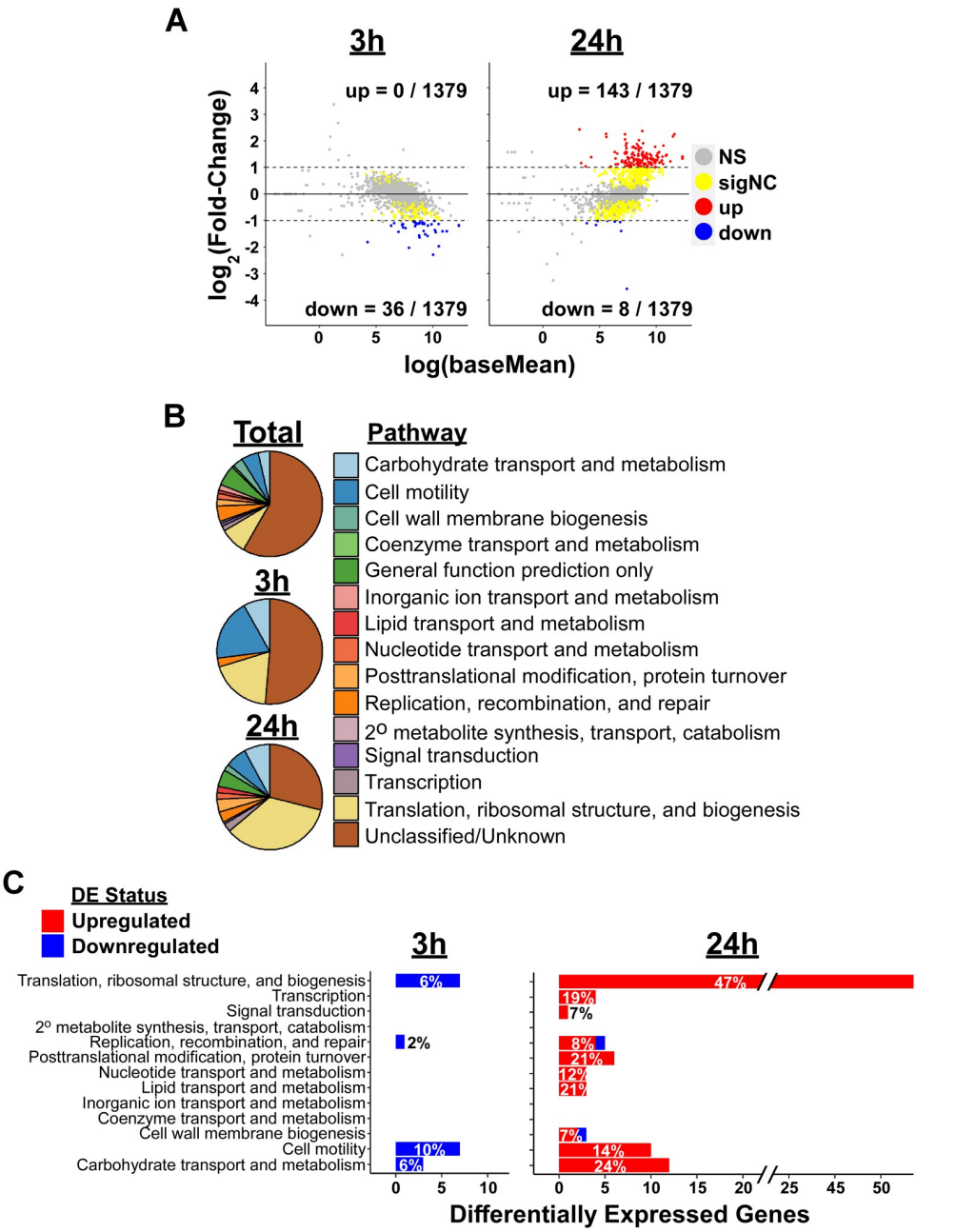

Fig 2. Doxycycline induced gene expression changes associated with protein translation. (A) Fold change versus expression strength for all detectable genes after 3 or 24 hours doxycycline treatment compared to untreated controls. Red (increased) and blue (decreased) dots represent genes with significantly different levels in treated vs. control bacteria ($\alpha = 0.05$, $\log_2$(fold-change) > 1). Yellow dots represent significantly different expression ($\alpha = 0.05$) without meeting our fold-change cutoff for differential expression ("sigNC"). Gray dots represent genes that were not significantly different between treatment and control bacteria ("NS"). Numbers of significantly upregulated (up) and downregulated (down) genes are shown as proportions of all detectable genes. (B) Clusters of Orthologous Genes (COG) pathways displayed as proportion of all detectable genes ("Total") compared to differentially expressed genes after 3h or 24h of doxycycline treatment [47]. (C) Stacked bar graph showing the number of increased (red) and decreased (blue) genes in each COG pathway at 3h and 24h timepoints. Percentage of genes in each pathway that were differentially expressed is stated within each bar. Note: Unclassified and general function prediction not shown.

https://doi.org/10.1371/journal.pone.0274125.g002

Table 1. Differentially expressed genes in doxycycline treated *B. burgdorferi* versus untreated controls.

locus	Description	COG pathway	log_2(fold change)[a]	
			3h	24h
BB_0691	elongation factor G (fusA)	Translation ribosomal structure and biogenesis	-1.01	1.52
BB_0786	50S ribosomal protein L25/general stress protein Ctc	Translation ribosomal structure and biogenesis	-1.04	1.30
BB_0479	50S ribosomal protein L4 (rplD)	Translation ribosomal structure and biogenesis	-1.08	1.40
BB_0690	neutrophil activating protein A (napA)	Replication recombination and repair	-1.08	2.02
BB_0055	triosephosphate isomerase (tpiA)	Carbohydrate transport and metabolism	-1.08	1.38
BB_0328	family 5 extracellular solute-binding protein	Unclassified	-1.10	NS
BB_0428	hypothetical protein	Unclassified	-1.10	1.12
BB_0330	peptide ABC transporter substrate-binding protein	Unclassified	-1.11	NS
BB_J09	outer surface protein D (ospD)	Unclassified	-1.12	NS
BB_0383	basic membrane protein A (bmpA)	Cell motility	-1.13	NS
BB_0603	integral outer membrane protein p66 (p66)	Unclassified	-1.13	NS
BB_0715	cell division protein FtsA (ftsA)	Unclassified	-1.14	NS
BB_0651	protein translocase subunit YajC	Cell motility	-1.14	1.57
BB_0034	outer membrane protein P13	Unclassified	-1.14	1.77
BB_0387	30S ribosomal protein S12 (rpsL)	Translation ribosomal structure and biogenesis	-1.15	1.11
BB_A15	outer surface protein A (ospA)	Unclassified	-1.18	1.33
BB_0337	enolase (eno)	Carbohydrate transport and metabolism	-1.19	NS
BB_0650	hypothetical protein	Unclassified	-1.20	1.58
BB_A16	outer surface protein B (ospB)	Unclassified	-1.20	1.41
BB_0293	flagellar basal body rod protein FlgC (flgC)	Cell motility	-1.21	1.17
BB_0396	50S ribosomal protein L33 (rpmG)	Translation ribosomal structure and biogenesis	-1.26	1.91
BB_0090	V-type ATP synthase subunit K	Unclassified	-1.29	1.06
BB_0385	basic membrane protein D (bmpD)	Cell motility	-1.36	NS
BB_A74	outer membrane porin OMS28 (osm28)	Cell motility	-1.40	NS
BB_0147	flagellin (flaB)	Cell motility	-1.41	1.22
BB_r05	rna13 gene (16S)	Unclassified	-1.41	NS
BB_0054	protein-export membrane protein SecG (secG)	Cell motility	-1.43	1.26
BB_r02	rna8 gene (23S rrlA)	Unclassified	-1.44	1.18
BB_0243	glycerol-3-phosphate dehydrogenase	Unclassified	-1.52	NS
BB_0240	glycerol uptake facilitator	Carbohydrate transport and metabolism	-1.57	NS
BB_0386	30S ribosomal protein S7 (rpsG)	Translation ribosomal structure and biogenesis	-1.58	NS
BB_0465	hypothetical protein	Unclassified	-1.64	1.91
BB_r01	rna7 gene = BB r01	Unclassified	-1.81	1.38
BB_r04	rna10 gene (23S rrlB)	Unclassified	-1.97	1.40
BB_0631	hypothetical protein	Unclassified	-2.03	1.76
BB_0241	glycerol kinase (glpK)	Unclassified	-2.29	NS
rnaseP	rnaseP	Unclassified	NS	2.42
BB_0188	50S ribosomal protein L20 (rplT)	Translation ribosomal structure and biogenesis	NS	2.37
BB_P40	hypothetical protein	Unclassified	NS	2.26
BB_0649	chaperonin GroEL (groL)	Posttranslational modification protein turnover chaperones	NS	2.25
bsrW	bsrW	Unclassified	NS	2.25
BB_B29	PTS system transporter subunit IIBC	Carbohydrate transport and metabolism	NS	2.17
BB_0614	hypothetical protein	Unclassified	NS	2.14
BB_0741	chaperonin GroS (groS)	Posttranslational modification protein turnover chaperones	NS	2.05
BB_0501	30S ribosomal protein S11 (rpsK)	Translation ribosomal structure and biogenesis	NS	1.88
BB_0780	50S ribosomal protein L27 (rpmA)	Translation ribosomal structure and biogenesis	NS	1.82

(*Continued*)

Table 1. (Continued)

locus	Description	COG pathway	log_2(fold change)[a]	
			3h	24h
BB_0445	fructose-bisphosphate aldolase (fbaA)	Carbohydrate transport and metabolism	NS	1.82
BB_0393	50S ribosomal protein L11 (rplK)	Translation ribosomal structure and biogenesis	NS	1.79
BB_A62	6.6 kDa lipoprotein (lp6.6)	Unclassified	NS	1.78
BB_0503	50S ribosomal protein L17 (rplQ)	Translation ribosomal structure and biogenesis	NS	1.73
BB_0405	hypothetical protein	Unclassified	NS	1.73
BB_0778	50S ribosomal protein L21 (rplU)	Translation ribosomal structure and biogenesis	NS	1.72
BB_0482	30S ribosomal protein S19 (rpsS)	Translation ribosomal structure and biogenesis	NS	1.71
BB_0776	hypothetical protein	Unclassified	NS	1.69
BB_0559	PTS system glucose-specific transporter subunit IIA	Carbohydrate transport and metabolism	NS	1.61
BB_O27	protein BdrN (bdrN)	Unclassified	NS	1.58
BB_0238	hypothetical protein	General function prediction only	NS	1.58
BB_0057	glyceraldehyde 3-phosphate dehydrogenase (gap)	Carbohydrate transport and metabolism	NS	1.57
BB_0489	50S ribosomal protein L24 (rplX)	Translation ribosomal structure and biogenesis	NS	1.55
BB_0113	30S ribosomal protein S18 (rpsR)	Translation ribosomal structure and biogenesis	NS	1.55
BB_0781	GTPase Obg	General function prediction only	NS	1.53
BB_0779	hypothetical protein	Translation ribosomal structure and biogenesis	NS	1.52
BB_0189	50S ribosomal protein L35 (rpmI)	Translation ribosomal structure and biogenesis	NS	1.52
BB_0488	50S ribosomal protein L14 (rplN)	Translation ribosomal structure and biogenesis	NS	1.52
BB_0802	ribosome-binding factor A (rbfA)	Translation ribosomal structure and biogenesis	NS	1.51
BB_0392	50S ribosomal protein L1 (rplA)	Translation ribosomal structure and biogenesis	NS	1.50
BB_0502	DNA-directed RNA polymerase subunit alpha (rpoA)	Transcription	NS	1.50
BB_0114	single-stranded DNA-binding protein	Replication recombination and repair	NS	1.50
BB_0366	aminopeptidase	Unclassified	NS	1.49
BB_0115	30S ribosomal protein S6	Translation ribosomal structure and biogenesis	NS	1.49
BB_0805	polyribonucleotide nucleotidyltransferase	Translation ribosomal structure and biogenesis	NS	1.47
BB_0485	50S ribosomal protein L16 (rplP)	Translation ribosomal structure and biogenesis	NS	1.46
BB_0695	30S ribosomal protein S16 (rpsP)	Translation ribosomal structure and biogenesis	NS	1.46
BB_0500	30S ribosomal protein S13 (rpsM)	Translation ribosomal structure and biogenesis	NS	1.45
BB_0390	50S ribosomal protein L7/L12 (rplL)	Translation ribosomal structure and biogenesis	NS	1.45
BB_0504	ribonuclease Y	General function prediction only	NS	1.44
BB_0476	elongation factor Tu (tuf)	Translation ribosomal structure and biogenesis	NS	1.44
BB_0348	pyruvate kinase (pyk)	Carbohydrate transport and metabolism	NS	1.43
BB_0699	50S ribosomal protein L19 (rplS)	Translation ribosomal structure and biogenesis	NS	1.43
BB_0558	phosphoenolpyruvate-protein phosphatase (ptsP)	Carbohydrate transport and metabolism	NS	1.40
BB_0128	cytidylate kinase (cmk)	Nucleotide transport and metabolism	NS	1.38
BB_0785	septation protein SpoVG (spoVG)	Cell wall membrane biogenesis	NS	1.38
BB_0478	50S ribosomal protein L3 (rplC)	Translation ribosomal structure and biogenesis	NS	1.38
BB_0493	50S ribosomal protein L6	Translation ribosomal structure and biogenesis	NS	1.37
BB_0069	aminopeptidase II	Unclassified	NS	1.37
BB_0394	transcription termination/antitermination factor (nusG)	Transcription	NS	1.35
BB_0283	flagellar hook protein FlgE (flgE)	Cell motility	NS	1.34
BB_0494	50S ribosomal protein L18 (rplR)	Translation ribosomal structure and biogenesis	NS	1.34
BB_0495	30S ribosomal protein S5 (rpsE)	Translation ribosomal structure and biogenesis	NS	1.34
BB_0229	50S ribosomal protein L31 type B (rpmE)	Translation ribosomal structure and biogenesis	NS	1.33
BB_0269	ATP-binding protein	Unclassified	NS	1.33
BB_0112	50S ribosomal protein L9 (rplI)	Translation ribosomal structure and biogenesis	NS	1.32

(*Continued*)

Table 1. (Continued)

locus	Description	COG pathway	log_2(fold change)[a]	
			3h	24h
BB_0683	3-hydroxy-3-methylglutaryl-CoA synthase	Lipid transport and metabolism	NS	1.32
BB_0087	L-lactate dehydrogenase	Unclassified	NS	1.30
BB_0477	30S ribosomal protein S10 (rpsJ)	Translation ribosomal structure and biogenesis	NS	1.30
BB_0047	hypothetical protein	Unclassified	NS	1.30
BB_0355	transcription factor	Transcription	NS	1.30
BB_0277	flagellar motor switch protein FliN (fliN)	Cell motility	NS	1.29
BB_0481	50S ribosomal protein L2 (rplB)	Translation ribosomal structure and biogenesis	NS	1.29
BB_0658	23-bisphosphoglycerate-dependent phosphoglycerate mutase	Carbohydrate transport and metabolism	NS	1.29
BB_0570	chemotaxis response regulator	Signal transduction mechanisms	NS	1.28
BB_0436	DNA gyrase subunit B (gyrB)	Replication recombination and repair	NS	1.28
BB_0483	50S ribosomal protein L22 (rplV)	Translation ribosomal structure and biogenesis	NS	1.27
BB_0056	phosphoglycerate kinase (pgk)	Carbohydrate transport and metabolism	NS	1.26
BB_0841	arginine deiminase (arcA)	Unclassified	NS	1.26
BB_0539	hypothetical protein	General function prediction only	NS	1.26
BB_0694	signal recognition particle protein (ffh)	Cell motility	NS	1.26
BB_0557	phosphocarrier protein HPr	Carbohydrate transport and metabolism	NS	1.24
BB_0777	adenine phosphoribosyltransferase (apt)	Nucleotide transport and metabolism	NS	1.24
BB_0127	30S ribosomal protein S1	Translation ribosomal structure and biogenesis	NS	1.24
BB_0122	elongation factor Ts (tsf)	Translation ribosomal structure and biogenesis	NS	1.22
BB_0789	ATP-dependent zinc metalloprotease FtsH	Posttranslational modification protein turnover chaperones	NS	1.21
BB_0492	30S ribosomal protein S8 (rpsH)	Translation ribosomal structure and biogenesis	NS	1.21
BB_0704	acyl carrier protein (acpP)	Lipid transport and metabolism	NS	1.21
BB_0104	periplasmic serine protease DO	Posttranslational modification protein turnover chaperones	NS	1.21
BB_0426	nucleoside 2-deoxyribosyltransferase superfamily protein	Function unknown	NS	1.20
BB_0027	hypothetical protein	Unclassified	NS	1.20
BB_0123	30S ribosomal protein S2 (rpsB)	Translation ribosomal structure and biogenesis	NS	1.20
BB_B19	outer surface protein C (ospC)	Unclassified	NS	1.18
BB_0727	phosphofructokinase	Carbohydrate transport and metabolism	NS	1.18
BB_0697	ribosome maturation factor RimM (rimM)	Translation ribosomal structure and biogenesis	NS	1.18
BB_B22	guanine/xanthine permease	General function prediction only	NS	1.17
BB_0061	thioredoxin (trx)	Posttranslational modification protein turnover chaperones	NS	1.17
BB_0338	30S ribosomal protein S9 (rpsI)	Translation ribosomal structure and biogenesis	NS	1.17
BB_0499	50S ribosomal protein L36 (rpmJ)	Translation ribosomal structure and biogenesis	NS	1.16
BB_0121	ribosome recycling factor (frr)	Translation ribosomal structure and biogenesis	NS	1.16
BB_0744	p83/100 antigen (p83/100)	Unclassified	NS	1.16
BB_0172	von Willebrand factor type A domain-containing protein	Function unknown	NS	1.16
BB_0615	30S ribosomal protein S4 (rpsD)	Translation ribosomal structure and biogenesis	NS	1.15
BB_0391	50S ribosomal protein L10	Translation ribosomal structure and biogenesis	NS	1.14
BB_0190	translation initiation factor IF-3 (infC)	Translation ribosomal structure and biogenesis	NS	1.14
BB_0059	CBS domain-containing protein	General function prediction only	NS	1.14
BB_0698	tRNA (guanine-N(1)-)-methyltransferase (trmD)	Translation ribosomal structure and biogenesis	NS	1.13
BB_0435	DNA gyrase subunit A (gyrA)	Replication recombination and repair	NS	1.13
BB_0735	rare lipoprotein A	Cell wall membrane biogenesis	NS	1.12
BB_0120	isoprenyl transferase (uppS)	Lipid transport and metabolism	NS	1.12
BB_0518	chaperone protein DnaK (dnaK)	Posttranslational modification protein turnover chaperones	NS	1.12
BB_0684	isopentenyl-diphosphate delta-isomerase (fni)	Unclassified	NS	1.12

(*Continued*)

Table 1. (Continued)

locus	Description	COG pathway	log_2(fold change)[a]	
			3h	24h
BB_0487	30S ribosomal protein S17 (rpsQ)	Translation ribosomal structure and biogenesis	NS	1.11
BB_0231	hypothetical protein	Function unknown	NS	1.10
BB_0020	diphosphate—fructose-6-phosphate 1-phosphotransferase	Carbohydrate transport and metabolism	NS	1.10
BB_0339	50S ribosomal protein L13 (rplM)	Translation ribosomal structure and biogenesis	NS	1.09
BB_0144	glycine/betaine ABC transporter substrate-binding protein	Unclassified	NS	1.09
BB_0588	MTA/SAH nucleosidase	Nucleotide transport and metabolism	NS	1.08
BB_0125	hypothetical protein	Unclassified	NS	1.07
BB_0230	transcription termination factor Rho (rho)	Transcription	NS	1.06
BB_0497	50S ribosomal protein L15 (rplO)	Translation ribosomal structure and biogenesis	NS	1.06
BB_0611	ATP-dependent Clp protease proteolytic subunit (clpP)	Cell motility	NS	1.06
BB_0842	ornithine carbamoyltransferase (argF)	Unclassified	NS	1.05
BB_0171	hypothetical protein	General function prediction only	NS	1.04
BB_0533	protein PhnP	General function prediction only	NS	1.04
BB_0491	30S ribosomal protein S14 (rpsN)	Translation ribosomal structure and biogenesis	NS	1.03
BB_0652	protein translocase subunit SecD (secD)	Cell motility	NS	1.01
BB_0281	motility protein A (motA)	Cell motility	NS	1.01
BB_0484	30S ribosomal protein S3 (rpsC)	Translation ribosomal structure and biogenesis	NS	1.01
BB_0070	hypothetical protein	Function unknown	NS	1.00
BB_0067	peptidase	Unclassified	NS	1.00
BB_0460	lipoprotein	Unclassified	NS	-1.01
BB_J46	hypothetical protein	Replication recombination and repair	NS	-1.02
BB_M37	protein BppC (bppC)	Unclassified	NS	-1.04
BB_0546	hypothetical protein	Cell wall membrane biogenesis	NS	-1.06
BB_M14	hypothetical protein	Unclassified	NS	-1.10
BB_F14	hypothetical protein	Unclassified	NS	-1.17
BB_L41	hypothetical protein	Unclassified	NS	-1.40
tmRNA	tmRNA	Unclassified	NS	-3.57

Fold changes are expressed as log_2. NS = not a significant change

[a]"NS" denotes not significantly different ($\alpha = 0.05$; log_2(fold change)>1)

https://doi.org/10.1371/journal.pone.0274125.t001

After 24 hours of doxycycline treatment, microscopical examination showed that *B. burgdorferi* were motile and were, therefore, metabolically active. RNA-Seq analyses at that time point revealed that 151 genes were differentially expressed (143 upregulated, 8 downregulated) compared to control cells (Fig 2A, Table 1, and S1 Table). Notably, a plurality of differentially expressed genes (53/151 DEGs; 35%) are involved in protein synthesis, all of which were upregulated in the treatment group (Fig 2B and 2C). These genes account for nearly half (47%) of all genes annotated as belonging to the translation, ribosomal structure, and biogenesis pathway (Fig 2C) [47]. These gene expression changes indicate that *B. burgdorferi* possesses a genetically-encoded mechanism(s) that attempts to overcome ribosome impairment, which is focused on enhanced production of mRNAs for components of translation.

The most common mechanism of bacterial resistance to tetracyclines is through efflux pumps that export the antibiotic from the cell [48]. While *B. burgdorferi* naturally encodes an efflux pump, BesCAB [49], levels of *besCAB* mRNA were not affected by presence of doxycycline (Table 1 and S1 Table). *B. burgdorferi* does not encode homologues of any known enzyme

that could modify doxycycline [50, 51], so that possible mechanism is unlikely to affect survival in the presence of the antibiotic.

Notably, expression of *napA* increased after 24h exposure to doxycycline (Table 1). This transcript encodes a periplasmic protein (also called BicA) that can bind copper and manganese, and associates with cell wall peptidoglycan [52–54]. The predicted sequence of NapA is similar to the Dps proteins of other bacterial species, which are involved with protecting DNA from stresses [55], although borrelia NapA lacks the Dps sequences that are involved with DNA-binding [52]. NapA derives its name from **n**eutrophil **a**ttracting **p**rotein **A**, and has been demonstrated to enhance immune responses [52, 54, 56–58]. It remains to be seen whether differential expressionof NapA occurs during doxycycline treatment in the context of mammalian infection.

As noted above, two other research groups have published results of RNA-Seq analyses of *B. burgdorferi* that were incubated for 5 days in 50 μg/ml doxycycline [45, 46]. The doxycycline concentration used in those studies was many times greater than what we and others found to inhibit *B. burgdorferi* replication in culture [44]. Although Feng et al. [45] described *B. burgdorferi* that had been incubated in 50 μg/ml doxycycline as "persisters", those researchers did not assess the viability of the bacteria that were used for RNA-Seq analysis. We also point out that the accepted definition of bacterial persistence cannot be applied to bacteriostatic antibiotics such as doxycycline, since the nature of those antibiotics does not directly kill bacteria [59]. The high dosages used by Feng at al. and Caskey et al. may explain why there is very little overlap between their results, despite both using essentially the same culture conditions [45, 46]. Feng et al. reported significant (> 2-fold) increases of 35 transcripts and decreases of 33 transcripts, encoding a broad range of functions [45]. In contrast, Caskey et al. [46] noted increases of 20 transcripts, while 40 transcripts were found to be downregulated. Many of the downregulated transcripts were of various plasmid encoded outer surface proteins. Of the 20 upregulated transcripts reported by Caskey et al., all but one came from the Lyme spirochete's resident cp32 prophages [60]. This is unlike the broad-ranging transcript groups reported to be upregulated by Feng et al. It is not clear whether the Caskey et al. results can be interpreted to imply anything about the native prophage's responses to doxycycline stress, since the vast majority of prophage genes were not affected. The increased transcripts encode portal proteins of four different cp32 bacteriophages, and three different Erp lipoproteins that localize to the bacteria's outer surface, are not predicted to be components of the bacteriophage particle, and do not possess functions relevant to survival in doxycycline [60–64].

Caskey et al. found that some bacteria had survived incubation for 5 days in 50μg/ml doxycycline, and resumed growth when subcultured in fresh medium without antibiotic or injected into mice [46]. That result is consistent with our observations of continued bacterial motility when exposed to 0.2 μg/ml doxycycline. As with other bacterial species, tetracyclines are bacteriostatic to *B. burgdorferi*, rather than overtly bactericidal [65].

Amoxicillin resulted in morphological changes, but not changes in gene expression

Amoxicillin is a β-lactam, which inhibits cell wall production. In contrast to doxycycline, exposure for 3 or 24 hours to 0.2 μg/ml amoxicillin did not result in significant changes to any transcript, even without a fold-change cutoff for differential expression designation (Fig 3 and S1 Table). The previous study by Feng et al. [45] reported that 5 days incubation in 50 μg/ml amoxicillin resulted in their detection of significant increases in 41 mRNAs of a range of functions, but none of which encode proteins involved with cell wall or membrane synthesis or

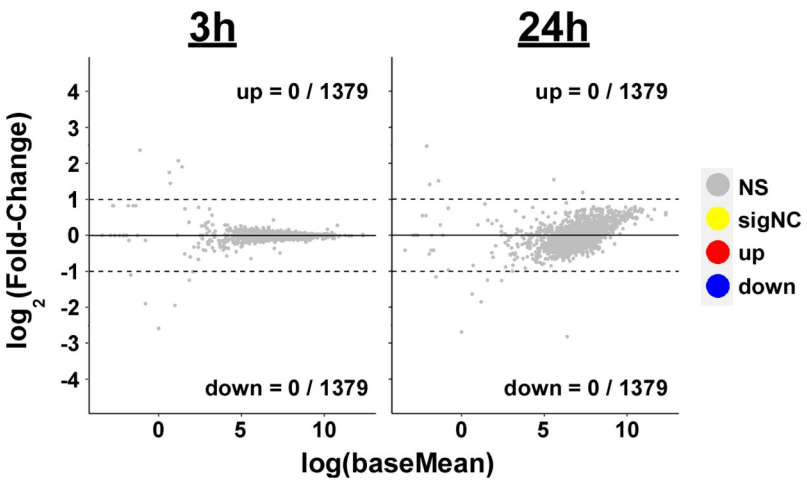

Fig 3. Amoxicillin did not induce gene expression changes. Fold change versus expression strength for all detectable genes after 3 or 24 hours amoxicillin treatment compared to untreated controls. No genes were significantly different between treatment and control groups (α = 0.05), as indicated by gray dots ("NS").

https://doi.org/10.1371/journal.pone.0274125.g003

remodeling. As noted above, Feng et al. did not assess bacterial viability before their RNA-Seq analyses.

The absence of cell wall-directed responses to amoxicillin suggests that *B. burgdorferi* may lack a mechanism to assess cell wall integrity. While many bacterial species recycle peptidoglycan components as they grow in size, *B. burgdorferi* lacks such an ability, and instead sheds remnants of cell wall remodeling into the environment [66]. Together, these suggest that *B. burgdorferi* transports peptidoglycan components into the periplasm to build its cell wall as it grows in length, while "assuming" that the cell wall is being assembled correctly.

Examination under the microscope revealed that amoxicillin-treated *B. burgdorferi* displayed evidence of membrane swelling (Fig 4). After 24 h in the antibiotic, microscopical examination of randomly selected bacteria showed membrane distensions in 49/110 (44.6%)

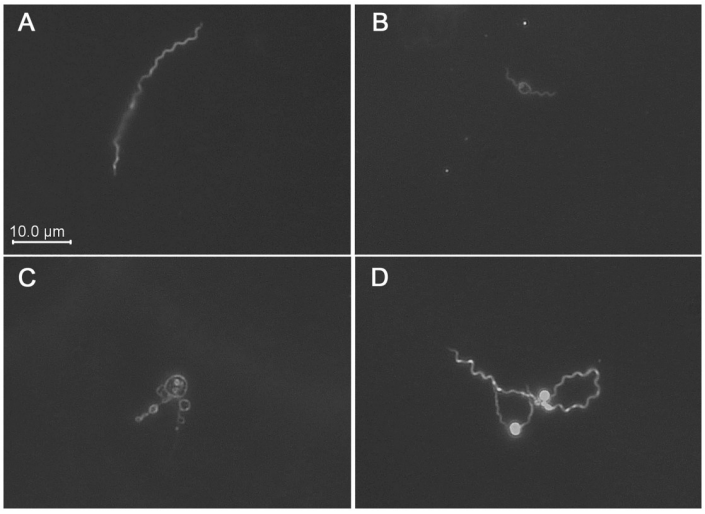

Fig 4. Photomicrographs of representative *B. burgdorferi* from (A) control, or (B, C, and D) amoxicillin-treated cultures after 24h incubation. All fields are shown at the same relative magnification. Imaged with a 40x objective lens and darkfield illumination.

https://doi.org/10.1371/journal.pone.0274125.g004

of amoxicillin-treated spirochetes, as compared to 6/109 (5.5%) of control *B. burgdorferi*. Those bacteria were comparable in shape to the so-called "round bodies" or "cysts" that have previously been described upon treatment of cultured *B. burgdorferi* with sublethal concentrations of β-lactams [13, 14, 16, 18, 33]. However, our transcriptomic analyses indicate that the amoxicillin-induced morphological changes were not genetically encoded. Instead, the observed membrane swellings were probably results of water diffusing into the cytoplasm and expanding the inner membrane that was no longer constrained by an intact cell wall. Similar osmotically-induced spheroplasts can be generated in other bacterial species through β-lactam induced weakening of their cell walls [19–22]. Although β-lactam derived spheroplasts of *B. burgdorferi* are evidently not biologically relevant to these bacteria in nature, such experimentally-derived structures can be useful for investigations of membrane functions [21, 22].

Conclusions

In nature, the Lyme disease spirochete exists only within vertebrates or ticks. In those environments, it is unlikely that *B. burgdorferi* would routinely encounter molds that produce β-lactam antibiotics and thus would not have been under pressure to evolve escape strategies. The evident inability of *B. burgdorferi* to respond to amoxicillin's inhibition of cell wall synthesis supports that hypothesis. Our data also suggest that *B. burgdorferi* does not naturally encounter other conditions that block peptidoglycan synthesis, and thus has not evolved mechanisms to respond to such a stress.

In contrast, *B. burgdorferi* evidently possesses a mechanism(s) that detects the impairment of translation due to doxycycline, and attempts to overcome that inhibition by increasing expression of genes involved with translation. Tetracyclines are synthesized in nature by actinomycete bacteria, which are predominantly soil microbes and are therefore unlikely to be encountered by *B. burgdorferi* in nature [67]. It remains to be seen whether other methods that inhibit translation yield similar effects. Nonetheless, the response of *B. burgdorferi* raises questions about where these spirochetes encounter translational impairment in their natural tick-vertebrate infectious cycle. One possibility is in the midgut of an unfed tick, where *B. burgdorferi* is starved for amino acids; accumulation of mRNAs for producing translation-associated proteins might allow rapid production of those proteins when the tick begins feeding on nutrient-rich blood. Further studies of Lyme disease spirochete physiology during its infectious cycle can help solve this question.

Taken together, our studies found that *B. burgdorferi* demonstrates distinct responses to different antibiotics. While it may be that *B. burgdorferi* within vertebrate tissues activate regulatory pathways that are not observed in culture, and thereby adapt to tolerate antibiotics, we also note that there is no direct evidence to support such hypothetical mechanisms. Importantly, neither our studies or those of Feng at al. or Caskey et al. [45, 46] directly addressed the efficacy of doxycycline or amoxycillin for treatment of Lyme disease in humans, as those treatments have been determined empirically. Rather, these insights shed light on the feedback mechanisms to environmental stresses by *B. burgdorferi*, and could lead to the development of novel therapeutic treatments for this important pathogen.

Supporting information

S1 Table. All results for doxycycline after 3h and 24h, and all results for amoxicillin after 3h and 24h.
(XLSX)

Acknowledgments

We thank Tatiana Castro-Padovani, Nerina Jusufovic, and Andrew Krusenstjerna for helpful comments on these studies and the manuscript.

Author Contributions

Conceptualization: Wolfram R. Zückert, Brian Stevenson.

Data curation: Timothy C. Saylor, Timothy Casselli, Catherine A. Brissette, Wolfram R. Zückert, Brian Stevenson.

Formal analysis: Timothy C. Saylor, Timothy Casselli, Jessamyn P. Moore, Katie M. Owens, Catherine A. Brissette, Wolfram R. Zückert, Brian Stevenson.

Funding acquisition: Catherine A. Brissette, Wolfram R. Zückert, Brian Stevenson.

Investigation: Timothy C. Saylor, Kathryn G. Lethbridge, Jessamyn P. Moore, Katie M. Owens.

Methodology: Timothy C. Saylor, Timothy Casselli, Wolfram R. Zückert, Brian Stevenson.

Project administration: Catherine A. Brissette, Wolfram R. Zückert, Brian Stevenson.

Resources: Catherine A. Brissette, Wolfram R. Zückert, Brian Stevenson.

Supervision: Brian Stevenson.

Validation: Timothy Casselli, Jessamyn P. Moore, Katie M. Owens.

Visualization: Timothy Casselli, Brian Stevenson.

Writing – original draft: Brian Stevenson.

Writing – review & editing: Timothy C. Saylor, Timothy Casselli, Catherine A. Brissette, Wolfram R. Zückert, Brian Stevenson.

References

1. Steere AC, Strle F, Wormser GP, Hu LT, Branda JA, Hovius JWR, et al. Lyme borreliosis. Nat Rev Dis Primers. 2016; 2:16090. https://doi.org/10.1038/nrdp.2016.90 PMID: 27976670
2. Kullberg BJ, Vrijmoeth HD, van de Schoor F, Hovius JW. Lyme borreliosis: diagnosis and management. Brit Med J. 2020; 369:m1041. https://doi.org/10.1136/bmj.m1041 PMID: 32457042
3. Centers for Disease Control and Prevention. Three sudden cardiac deaths associated with Lyme carditis—United States, November 2012-July 2013. Morb Mortal Wkly Rep. 2013; 62:993–6. PMID: 24336130
4. Wormser GP, Dattwyler RJ, Shapiro ED, Halperin JJ, Steere AC, Klempner MS, et al. The clinical assessment, treatment, and prevention of Lyme disease, human granulocytic anaplasmosis, and babesiosis: Clinical practice guidelines by the Infectious Diseases Society of America. Clin Infect Dis. 2006; 43:1089–134. https://doi.org/10.1086/508667 PMID: 17029130
5. Sanchez E, Vannier E, Wormser GP, Hu LT. Diagnosis, treatment, and prevention of Lyme disease, human granulocytic anaplasmosis, and babesiosis: a review. JAMA. 2016; 315:1767–77. https://doi.org/10.1001/jama.2016.2884 PMID: 27115378
6. Centers for Disease Control and Prevention. Treatment for erythema migrans [cited 2021 December]. https://www.cdc.gov/lyme/treatment/index.html.
7. Lobritz MA, Belenky P, Porter CB, Gutierrez A, Yang JH, Schwarz EG, et al. Antibiotic efficacy is linked to bacterial cellular respiration. Proc Natl Acad Sci. 2015; 112:8173–80. https://doi.org/10.1073/pnas.1509743112 PMID: 26100898
8. Mueller EA, Levin PA. Bacterial cell wall quality control during environmental stress. mBio. 2020; 11: e02456–20. https://doi.org/10.1128/mBio.02456-20 PMID: 33051371
9. Cardoza E, Singh H. C group-mediated antibiotic stress mimics the cold shock response. Curr Microbiol. 2021; 78:3372–80. https://doi.org/10.1007/s00284-021-02613-7 PMID: 34283283

10. Wüllner D, M. G, Haupt A, Liang X, P/ Z, Dietze P, et al. Adaptive responses of *Pseudomonas aeruginosa* to treatment with antibiotics. Antimicrob Agents Chemother. 2022; 66:e0087821.
11. Cho H, Uehara T, Bernhardt TG. Beta-lactam antibiotics induce a lethal malfunctioning of the bacterial cell wall synthesis machinery. Cell. 2014; 159:1300–11. https://doi.org/10.1016/j.cell.2014.11.017 PMID: 25480295
12. Flores-Kim J, Dobihal GS, Fenton A, Rudner DZ, Bernhardt TG. A switch in surface polymer biogenesis triggers growth-phase-dependent and antibiotic-induced bacteriolysis. eLife. 2019; 8:e44912. https://doi.org/10.7554/eLife.44912 PMID: 30964003
13. Schaller M, Neubert U. Ultrastructure of *Borrelia burgdorferi* after exposure to benzylpenicillin. Infection. 1994; 22:401–6.
14. Kersten A, Poitschek C, Rauch S, Aberer E. Effects of penicillin, ceftriaxone, and doxycycline on morphology of *Borrelia burgdorferi*. Antimicrob Agents Chemother. 1995; 39:1127–33.
15. Brorson Ø, Brorson SH. Transformation of cystic forms of *Borrelia burgdorferi* to normal, mobile spirochetes. Infection. 1997; 25:240–6.
16. Murgia R, Piazzetta C, Cinco M. Cystic forms of *Borrelia burgdorferi* sensu lato: induction, development, and the role of RpoS. Wien Klin Wochenschr. 2002; 114:574–9.
17. Brorson Ø, Brorson SH, Scythes J, MacAllister J, Wier A, Margulis L. Destruction of spirochete *Borrelia burgdorferi* round-body propagules (RBs) by the antibiotic tigecycline. Proc Natl Acad Sci. 2009; 106:18656–61.
18. Feng J, Shi W, Zhang S, Sullivan D, Auwaerter PG, Zhang Y. A drug combination screen identifies drugs active against amoxicillin-induced round bodies of in vitro *Borrelia burgdorferi* persisters from an FDA drug library. Front Microbiol. 2016; 7:743.
19. Sun Y, Sun TL, Huang HW. Physical properties of *Escherichia coli* spheroplast membranes. Biophys J. 2014; 107:2082–90.
20. Cushnie TP, O'Driscoll NH, Lamb AJ. Morphological and ultrastructural changes in bacterial cells as an indicator of antibacterial mechanism of action. Cell Mol Life Sci. 2016; 73:4471–92. https://doi.org/10.1007/s00018-016-2302-2 PMID: 27392605
21. Nishida H. Factors that affect the enlargement of bacterial protoplasts and spheroplasts. Int J Mol Sci. 2020; 21:7131. https://doi.org/10.3390/ijms21197131 PMID: 32992574
22. Kaback HR. It's better to be lucky than smart. Annu Rev Biochem. 2021; 90:1–29. https://doi.org/10.1146/annurev-biochem-011520-105008 PMID: 33472005
23. Brorson Ø, Brorson SH. In vitro conversion of *Borrelia burgdorferi* to cystic forms in spinal fluid, and transformation to mobile spirochetes by incubation in BSK-H medium. Infection. 1998; 26:144–50.
24. Brorson Ø, Brorson SH. A rapid method for generating cystic forms of *Borrelia burgdorferi*, and their reversal to mobile spirochetes. APMIS. 1998; 106:1131–41.
25. Gruntar I, Malovrh T, Murgia R, Cinco M. Conversion of *Borrelia garinii* cystic forms to motile spirochetes in vivo. APMIS. 2001; 109:383–8.
26. MacDonald AB. Spirochetal cyst forms in neurodegenerative disorders,. . .hiding in plain sight. Med Hypotheses. 2006; 67:819–32. https://doi.org/10.1016/j.mehy.2006.04.025 PMID: 16828236
27. Stricker RB, Johnson L. Chronic Lyme disease and the 'Axis of Evil'. Future Microbiol. 2008; 3:621–4. https://doi.org/10.2217/17460913.3.6.621 PMID: 19072179
28. Stricker RB, Johnson L. Lyme disease: the next decade. Infect Drug Resist. 2011; 4:1–9. https://doi.org/10.2147/IDR.S15653 PMID: 21694904
29. Sapi E, Kaur N, Anyanwu S, Luecke DF, Datar A, Patel S, et al. Evaluation of in-vitro antibiotic susceptibility of different morphological forms of *Borrelia burgdorferi*. Infect Drug Resist. 2011; 4:97–113.
30. Lantos PM, Auwaerter PG, Wormser GP. A systematic review of *Borrelia burgdorferi* morphologic variants does not support a role in chronic Lyme disease. Clin Infect Dis. 2014; 58:663–71.
31. Sharma B, Brown AV, Matluck NE, Hu LT, Lewis K. *Borrelia burgdorferi*, the causative agent of Lyme disease, forms drug-tolerant persister cells. Antimicrob Agents Chemother. 2015; 59:4616–24.
32. Meriläinen L, Brander H, Herranen A, A. S, Gilbert L. Pleomorphic forms of *Borrelia burgdorferi* induce distinct immune responses. Microbes Infect. 2016; 18:484–95.
33. Rudenko N, Golovchenko M, Kybicova K, Vancova M. Metamorphoses of Lyme disease spirochetes: phenomenon of *Borrelia* persisters. Parasit Vectors. 2019; 12:237.
34. Cabello FC, Embers ME, Newman SA, Godfrey HP. *Borreliella burgdorferi* antimicrobial-tolerant persistence in Lyme disease and posttreatment Lyme disease syndromes. mBio. 2022:e0344021.
35. Miller JC, von Lackum K, Babb K, McAlister JD, Stevenson B. Temporal analysis of *Borrelia burgdorferi* Erp protein expression throughout the mammal-tick infectious cycle. Infect Immun. 2003; 71:6943–52.

36. Zückert WR. Laboratory maintenance of *Borrelia burgdorferi*. Curr Protoc Microbiol. 2007; 12C:1–10.

37. Coenye T. Do results obtained with RNA-sequencing require independent verification? Biofilm. 2021; 3:100043. https://doi.org/10.1016/j.bioflm.2021.100043 PMID: 33665610

38. Arnold WK, Savage CR, Brissette CA, Seshu J, Livny J, Stevenson B. RNA-Seq of *Borrelia burgdorferi* in multiple phases of growth reveals insights into the dynamics of gene expression, transcriptome architecture, and noncoding RNAs. PLoS One. 2016; 11:e0164165.

39. Arnold WK, Savage CR, Lethbridge KG, Smith TC, Brissette CA, Seshu J, et al. Transcriptomic insights on the virulence-controlling CsrA, BadR, RpoN, and RpoS regulatory networks in the Lyme disease spirochete. PLoS One. 2018; 13:e0203286. https://doi.org/10.1371/journal.pone.0203286 PMID: 30161198

40. Casselli T, Tourand Y, Scheidegger A, Arnold WK, Proulx A, Stevenson B, et al. DNA methylation by restriction modification systems affects the global transcriptome profile in *Borrelia burgdorferi*. J Bacteriol. 2018; 200:e00395–18.

41. Bolger AM, Lohse M, Usadel B. Trimmomatic: a flexible trimmer for Illumina sequence data. Bioinformatics. 2014; 30:2114–20. https://doi.org/10.1093/bioinformatics/btu170 PMID: 24695404

42. Patro R, Duggal G, Love MI, Irizarry RA, Kingsford C. Salmon provides fast and bias-aware quantification of transcript expression. Nat Methods. 2017; 14:417–9. https://doi.org/10.1038/nmeth.4197 PMID: 28263959

43. Love MI, Huber W, Anders S. Moderated estimation of fold change and dispersion for RNA-seq data with DESeq2. Genome Biol. 2014; 15:550. https://doi.org/10.1186/s13059-014-0550-8 PMID: 25516281

44. Sicklinger M, Wienecke R, Neubert U. In vitro susceptibility testing of four antibiotics against *Borrelia burgdorferi*: a comparison of results for the three genospecies *Borrelia afzelii*, *Borrelia garinii*, and *Borrelia burgdorferi* sensu stricto. J Clin Microbiol. 2003; 41:1791–3.

45. Feng J, Shi W, Zhang S, Zhang Y. Persister mechanisms in *Borrelia burgdorferi*: implications for improved intervention. Emerg Microbes Infect. 2015; 4:e51.

46. Caskey JR, Hasenkampf NR, Martin DS, Chouljenko VN, Subramanian R, Cheslock MA, et al. The functional and molecular effects of doxycycline treatment on *Borrelia burgdorferi* phenotype. Front Microbiol. 2019; 10:690.

47. Galperin MY, Makarova KS, Wolf YI, Koonin EV. Expanded microbial genome coverage and improved protein family annotation in the COG database. Nucleic Acids Res. 2015; 43:D261–9. https://doi.org/10.1093/nar/gku1223 PMID: 25428365

48. Chopra I. Genetic and biochemical basis of tetracycline resistance. J Antimicrob Chemother. 1986; 18 Suppl C:51–6. https://doi.org/10.1093/jac/18.supplement_c.51 PMID: 3542941

49. Bunikis I, Denker K, Ostberg Y, Andersen C, Benz R, Bergström S. An RND-type efflux system in *Borrelia burgdorferi* is involved in virulence and resistance to antimicrobial compounds. PLoS Pathog. 2008; 4:e1000009.

50. Fraser CM, Casjens S, Huang WM, Sutton GG, Clayton R, Lathigra R, et al. Genomic sequence of a Lyme disease spirochaete, *Borrelia burgdorferi*. Nature. 1997; 390:580–6.

51. Casjens S, Palmer N, van Vugt R, Huang WM, Stevenson B, Rosa P, et al. A bacterial genome in flux: the twelve linear and nine circular extrachromosomal DNAs of an infectious isolate of the Lyme disease spirochete *Borrelia burgdorferi*. Mol Microbiol. 2000; 35:490–516.

52. Codolo G, Papinutto E, Polenghi A, D'Elios MM, Zanotti G, de Bernard M. Structure and immunomodulatory property relationship in NapA of *Borrelia burgdorferi*. Biochim Biophys Acta. 2010; 1804:2191–7.

53. Wang P, Lutton A, Olesik J, Vali H, Li X. A novel iron- and copper-binding protein in the Lyme disease spirochaete. Mol Microbiol. 2012; 86:1441–51. https://doi.org/10.1111/mmi.12068 PMID: 23061404

54. Davis MM, Brock AM, DeHart TG, Boribong BP, Lee K, McClune ME, et al. The peptidoglycan-associated protein NapA plays an important role in the envelope integrity and in the pathogenesis of the Lyme disease spirochete. PLoS Pathog. 2021; 17:e1009546. https://doi.org/10.1371/journal.ppat.1009546 PMID: 33984073

55. Ishihama A. Modulation of the nucleoid, the transcription apparatus, and the translation machinery in bacteria for stationary phase survival. Genes to Cells. 1999; 4:135–43. https://doi.org/10.1046/j.1365-2443.1999.00247.x PMID: 10320479

56. Codolo G, Amedei A, Steere AC, Papinutto E, Cappon A, Polenghi A, et al. *Borrelia burgdorferi* NapA-driven Th17 cell inflammation in Lyme arthritis. Arthritis Rheum. 2008; 58:3609–17.

57. Amedei A, Codolo G, Ozolins D, Ballerini C, Biagioli T, Jaunalksne I, et al. Cerebrospinal fluid T-regulatory cells recognize *Borrelia burgdorferi* NapA in chronic Lyme borreliosis. Int J Immunopathol Pharmacol. 2013; 26:907–15.

58. Codolo G, Bossi F, Durigutto P, Bella CD, Fischetti F, Amedei A, et al. Orchestration of inflammation and adaptive immunity in *Borrelia burgdorferi*-induced arthritis by neutrophil-activating protein A. Arthritis Rheum. 2013; 65:1232–42.

59. Balaban NQ, Helaine S, Lewis K, Ackermann M, Aldridge B, Andersson DI, et al. Definitions and guidelines for research on antibiotic persistence. Nat Rev Microbiol. 2019; 17:441–8. https://doi.org/10.1038/s41579-019-0196-3 PMID: 30980069

60. Stevenson B, Zückert WR, Akins DR. Repetition, conservation, and variation: the multiple cp32 plasmids of *Borrelia* species. In: Saier MH, García-Lara J, editors. The Spirochetes: Molecular and Cellular Biology. Oxford: Horizon Press; 2001. p. 87–100.

61. Casjens S, van Vugt R, Tilly K, Rosa PA, Stevenson B. Homology throughout the multiple 32-kilobase circular plasmids present in Lyme disease spirochetes. J Bacteriol. 1997; 179:217–27. https://doi.org/10.1128/jb.179.1.217-227.1997 PMID: 8982001

62. Eggers CH, Samuels DS. Molecular evidence for a new bacteriophage of *Borrelia burgdorferi*. J Bacteriol. 1999; 181:7308–13.

63. Zhang H, Marconi RT. Demonstration of cotranscription and 1-methyl-3-nitroso-nitroguanidine induction of a 30-gene operon of *Borrelia burgdorferi*: evidence that the 32-kilobase circular plasmids are prophages. J Bacteriol. 2005; 187:7985–95.

64. Stevenson B, Bykowski T, Cooley AE, Babb K, Miller JC, Woodman ME, et al. The Lyme disease spirochete Erp lipoprotein family: structure, function and regulation of expression. In: Cabello FC, Godfrey HP, Hulinska D, editors. Molecular Biology of Spirochetes. Amsterdam: IOS Press; 2006. p. 354–72.

65. Smilack JD. The tetracyclines. Mayo Clin Proc. 1999; 74:727–9. https://doi.org/10.4065/74.7.727 PMID: 10405705

66. Jutras BL, Lochhead RB, Kloos ZA, Biboy J, Strle K, Booth CJ, et al. *Borrelia burgdorferi* peptidoglycan is a persistent antigen in patients with Lyme arthritis. Proc Natl Acad Sci USA. 2019; 116:13498–507.

67. Nelson ML, Levy SB. The history of the tetracyclines. Ann NY Acad Sci. 2011; 1241:17–32. https://doi.org/10.1111/j.1749-6632.2011.06354.x PMID: 22191524